Spectrochimica Acta Part A: Molecular and Biomolecular Spectroscopy 153 (2016) 397–401

Contents lists available at ScienceDirect

Spectrochimica Acta Part A: Molecular and Biomolecular Spectroscopy

journal homepage: www.elsevier.com/locate/saa

Benzimidazole based ratiometric and colourimetric chemosensor for Ni(II)

Deblina Sarkar, Ajoy Kumar Pramanik, Tapan Kumar Mondal *

Department of Chemistry, Jadavpur University, Kolkata 700032, India

ARTICLE INFO

Article history:
Received 2 June 2015
Received in revised form 13 August 2015
Accepted 30 August 2015
Available online 3 September 2015

Keywords:
Benzimidazole based chemosensor for Ni^{2+}
Colourimetric sensor
Spectral characterization
DFT calculation

ABSTRACT

A highly sensitive and selective benzimidazole based colourimetric chemosensor (HL) for the efficient detection of Ni^{2+} has been reported. The synthesized chemosensor HL is highly efficient in detecting Ni^{2+} over other metal ions that commonly coexist with Ni^{2+} in physiological and environmental samples. HL also shows distinct color change from orange yellow to blue visible under the naked eye due to specific binding with Ni^{2+}. This color change corresponds to a large red shift of the UV–Vis spectrum from 403 nm to 600 nm with a distinct isosbestic point at around 500 nm. The cation sensing property of the receptor HL has been examined by UV–Vis spectroscopy. Electronic structure of the HL–Ni^{2+} complex and sensing mechanism has been interpreted by DFT and TDDFT calculations.

1. Introduction

Nickel plays an important role in industrial field with widespread application in Ni–Cd batteries, electroplating, welding, painting pigments, as magnetic tapes in computers as well as catalyst in hydrogenation processes [1]. Nickel is also present in the active site of various enzymes, present in certain microorganisms and plants. However, it is a toxic metal from biological point of view resulting in pneumonitis, asthma, lung cancer and also certain disorder of the central nervous system as well as the respiratory system [2–7]. Thus detection of nickel is very important both from industrial as well as biological point of view. Though a number of techniques such as atomic absorption spectrometry (AAS), flame atomic absorption spectrometry–electro thermal atomization (AAS–ETA) [8,9], ICP-AES, and flame photometry are widely used for the detection of nickel but naked eye detection of the metal using a colorimetric as well as ratiometric sensor is quite demanding. Colourimetric detection of metal ion is very sensitive, rapid, and simple to-use method.

Although several organic molecules have been reported which exhibit the property of colourimetric sensing of nickel(II), yet the reported numbers are few. Domínguez et al. reported a Schiff base derivative of cinnamaldehyde used in the colourimetric detection of nickel(II) [10]. Jiang and Wang et al. reported coumarin based colourimetric chemosensors for the detection of nickel(II) [11,12], while S. Goswami et al. developed a quinoxaline based colourimetric and ratiometric chemosensor for specific detection of nickel(II) [13]. In this present work, report of a benzimidazole based colourimetric chemosensor for the detection of nickel(II) is quite an important addition to the library of few other organic molecules with this property of rapid detection of nickel(II).

The present work describes the colourimetric sensing property of a benzimidazole based organic framework for the rapid detection of nickel(II). Benzimidazoles are very useful intermediates for the development of molecules of biological interest. Benzimidazole and its derivatives have found applications in biological activities such as antimicrobial, anticancer, anti-inflammatory, antivirus and anticonvulsant [14–23]. The chemosensor HL has been synthesized using the procedure reported by D. Sarkar et al. [24]. Cation binding studies have been extensively studied by means of UV–Vis spectroscopy as well as by naked eye detection. The chemical, electronic structure and photophysical properties have been studied by various spectroscopic analyses abetted with DFT and TDDFT calculations.

2. Experimental

2.1. Materials and methods

2-Amino-4-methylphenol and benzimidazole were purchased from Aldrich. All other organic chemicals and inorganic salts were available from Sisco Research Lab, Mumbai, India and used without further purification. Commercially available SRL silica gel (60–120 mesh) was used for column chromatography.

Elemental analysis was carried out in a 2400 Series-II CHN analyzer, PerkinElmer, USA. HRMS mass spectra were recorded on Waters (Xevo G2 Q-TOF) mass spectrometer. Infrared spectra were taken on a RX-1 PerkinElmer spectrophotometer with samples prepared as KBr pellets. Electronic spectral studies were performed on a PerkinElmer Lambda

* Corresponding author.
E-mail address: tkmondal@chemistry.jdvu.ac.in (T.K. Mondal).

http://dx.doi.org/10.1016/j.saa.2015.08.052
1386-1425/

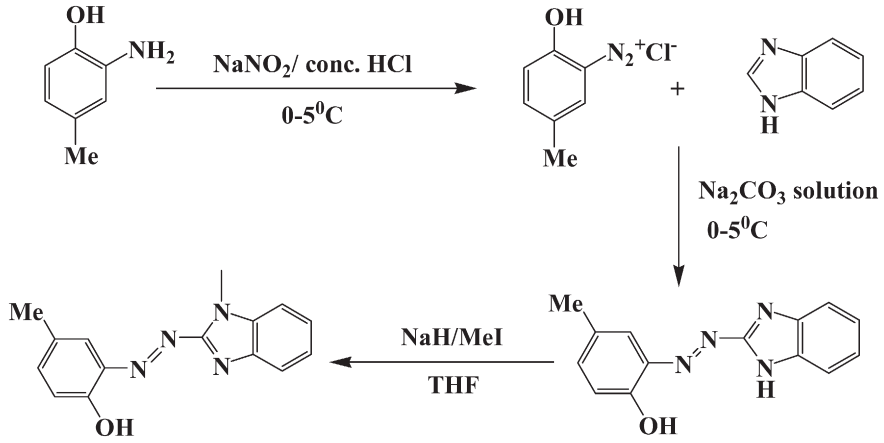

Scheme 1. Synthesis of benzimidazole based chemosensor HL.

750 spectrophotometer. NMR spectra were recorded using a Bruker (AC) 300 MHz FTNMR spectrometer of ~0.05 M solutions of the compounds in DMSO-d6.

2.2. Synthesis of 2-[(1-methyl-2-benzimidazolyl)azo]-p-cresol (HL)

The receptor HL has been synthesized using the reported procedure [24]. 2-Amino-4-methylphenol (4.0 g, 32.4 mmol) was dissolved in 10 mL 6(N) HCl and cooled to 0 °C. Sodium nitrite (2.8 g, 42.12 mmol) was dissolved in minimum volume of water and cooled to 0 °C. The diazotized solution was added dropwise with constant stirring to benzimidazole (4.0 g, 34.0 mmol) dissolved in aqueous solution of sodium carbonate (5.1 g, 48.0 mmol). The product was purified by column chromatography using silica gel (60–120 mesh) and eluted by 20% (v/v) ethyl acetate petroleum ether mixture. Yield was 5.1 g, 64%.

3.2 g (12.6 mmol) of the diazo-coupled product was taken and N-methylation was performed with MeI (1.8 g, 13.0 mmol) using NaH (1.0 g, 25.1 mmol) as base in dry THF medium following the reported methods [25]. The product was subjected to chromatographic separation on a silica gel column (60–120 mesh). The desired red band of HL was eluted with 10% (v/v) ethyl acetate petroleum ether mixture. Evaporation of the solvent under reduced pressure afforded pure compound. Yield was 2.1 g, 62%.

Anal. Calc. for $C_{15}H_{14}N_4O$ (HL): C, 67.65; H, 5.30; N, 21.04%. Found: C, 67.82; H, 5.32; N, 21.11%. IR data (KBr, cm^{-1}): 3373 υ(O–H); 1620 υ(C═N); 1419 υ(N═N). ^1H NMR data (DMSO-d_6, ppm): 13.56 (1H, s), 7.86 (1H, s), 7.81 (1H, d, $J = 7.7$ Hz), 7.69 (1H, d, $J = 8.2$ Hz), 7.38 (1H, d, $J = 7.4$ Hz), 7.21–7.35 (3H, m), 3.80 (3H, s), 2.13 (3H, s).

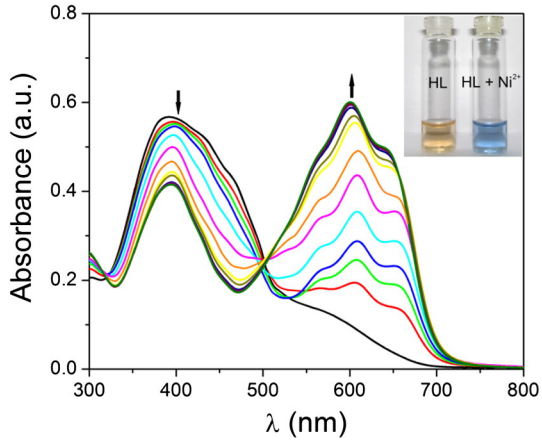

Fig. 1. Change in UV–Vis spectrum of HL (10 μM) upon gradual addition of 10 μM Ni^{2+}. Inset shows the visual effect of addition of Ni^{2+} to HL in ambient light.

2.3. General method for UV–Vis titration

2.3.1. UV–Vis method

Stock solution of the receptor HL (10 μM) in [(DMSO/H_2O), 1:1, v/v] (at 25 °C) using HEPES buffered solution at pH = 7.4 was prepared. The solution of the guest cations using their chloride salts in the order of 100 μM was prepared in deionized water. Solutions of various concentrations containing host and increasing concentrations of cations were prepared separately. The spectra of these solutions were recorded by means of UV–Vis methods.

2.3.2. Job's plot by UV–Vis method

A series of solutions containing HL (10 μM) and $NiCl_2$ (10 μM) were prepared in such a manner that the sum of the total metal ion and HL volume remained constant (5 mL). DMSO:H_2O (1:1, v/v) was used as solvent at pH 7.4 using HEPES buffer. Job's plots were drawn by plotting (A_0–A) versus mole fraction of Ni^{2+} at 403 nm and A–A_0 versus mole fraction of Ni^{2+} at 600 nm [A_0 = absorption intensity of the free receptor and A is the absorption intensity of HL after addition of Ni^{2+}].

2.3.3. Determination of limit of detection

The detection limit was calculated based on the UV–Vis titration. To determine the S/N ratio, the emission intensity of HL without any analyte was measured by 10 times and the standard deviation of blank measurements was found to be 2.79×10^{-3}. The limit of detection (LOD) of HL for Ni^{2+} was determined from the following equation: LOD = K × SD / S, where K = 3 in this case, SD is the standard deviation of the blank solution and S is the slope of the calibration curve. From the graph, we get slope = 0.56465×10^5, and SD value is 2.79×10^{-3}. Thus using the formula, we get the LOD = 0.14 μM.

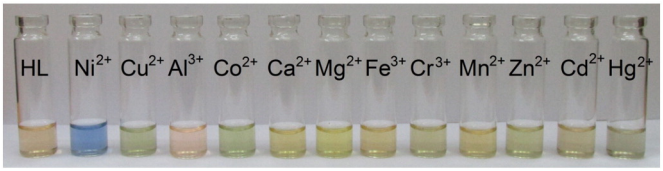

Fig. 2. Visual changes of HL with different metal ions in DMSO–HEPES buffer (1:1, v/v, pH 7.4) solution. (For interpretation of the references to color in this figure, the reader is referred to the web version of this article.)

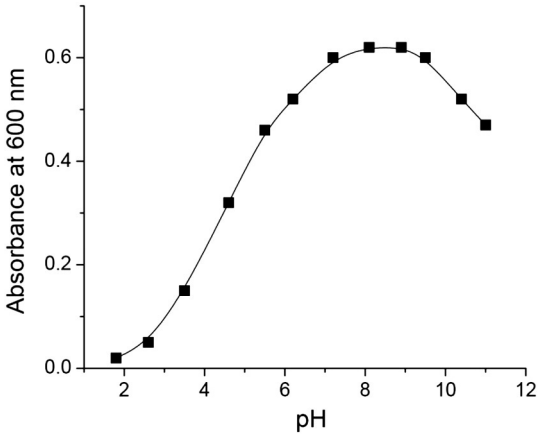

Fig. 3. Absorbance at 600 nm in DMSO/H_2O (1:1, v/v) with different pH.

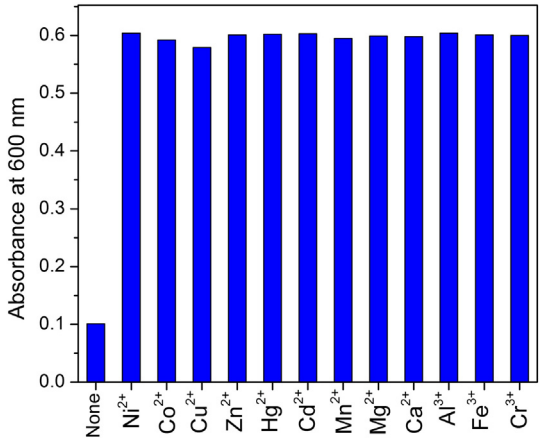

Fig. 5. Absorbance at 600 nm of HL (10 μM) in the presence of Ni^{2+} (10 μM) and other competing metal ions i.e. Ca^{2+}, Mg^{2+}, Mn^{2+}, Fe^{3+}, Al^{3+}, Cr^{3+}, Co^{2+}, Zn^{2+}, Cu^{2+}, Cd^{2+} and Hg^{2+} (20 μM) DMSO–HEPES buffer (1:1, v/v, pH 7.4) solution.

2.3.4. Determination of binding constant from UV–Vis titration data

Binding constant was calculated according to the Benesi–Hildebrand equation. K_a was calculated following the equation stated below.

$$1/(A–A_o) = 1/\{K_a(A_{max}–A_o)\,[Ni^{2+}]^n\} + 1/[A_{max}–A_o]$$

Here, A_o is the absorbance of receptor in the absence of guest, A is the absorbance recorded in the presence of added guest, A_{max} is the absorbance in the presence of added $[Ni^{2+}]_{max}$ and K_a is the association constant (M^{-1}). The association constant (K_a) could be determined from the slope of the straight line of the plot of $1/(A–A_o)$ against $1/[Ni^{2+}]^n$, here $n = 1$. The association constant (K_a) as determined by UV–Vis titration method for sensor with Ni^{2+}, is found to be $2.08 \times 10^5\ M^{-1}$.

2.4. Computational method

All computations were performed using the Gaussian09 (G09) program [26] in B3LYP method [27,28]. The 6–31 + G(d) basis set was assigned for C, H, N and O atoms [29]. The LANL2DZ basis set with effective core potential was employed for the Ni atom [30–32]. The vibrational frequency calculations were performed to ensure that the optimized geometries represent the local minima of potential energy surface and there are only positive eigen-values [33]. The lowest 40 singlet–singlet vertical electronic excitations based on B3LYP optimized geometries were computed using the time-dependent density functional theory (TDDFT) formalism [34–36] in DMSO for HL and HL–Ni^{2+} complex using conductor-like polarizable continuum model (CPCM) [37–39] with the same B3LYP level and basis sets.

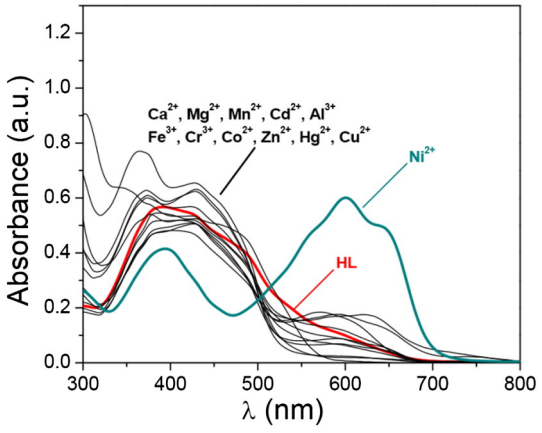

Fig. 4. UV–Vis spectra of chemosensor (HL) (10 μM) upon addition of various metal ions i.e. Ca^{2+}, Mg^{2+}, Mn^{2+}, Fe^{3+}, Al^{3+}, Cr^{3+}, Co^{2+}, Zn^{2+}, Cu^{2+}, Cd^{2+} and Hg^{2+} (20 μM).

3. Results and discussion

3.1. Synthesis and formulation

The receptor, 2-[(1-methyl-2-benzimidazolyl)azo]-p-cresol (HL) (Scheme 1) has been synthesized by coupling of diazotized 2-amino-4-methylphenol with benzimidazole in alkaline medium. The compound has been characterized by elemental and mass spectral analysis along with other spectroscopic techniques (IR, UV–Vis, NMR etc.) (see experimental section).

3.2. IR, NMR and mass spectral analyses

IR spectrum of the free receptor HL, show a broad stretching at 3373 cm^{-1} corresponding to υ(OH), the υ(C═N) and υ(N═N) appeared at 1620 and 1419 cm^{-1}. In the HL–Ni^{2+} complex, the band at 3373 cm^{-1} disappears due to co-ordination while the υ(C═N) and υ(N═N) appeared at 1594 and 1390 cm^{-1}. The HRMS spectrum of HL–Ni^{2+} complex shows a strong peak at 382.4 corresponding to $Na[Ni(L\text{-}H)Cl]^+$ species (Fig. S1) supporting 1:1 complex formation. In a square planar environment, three coordination sites are satisfied by the N, N, O donor of HL and the fourth site being occupied by a Cl^-. The square planar geometry of the complex is again supported by well resolved ^1H NMR spectrum. In the complex, the N-Me and $–CH_3$ protons appear at 3.85 and 2.19 (Fig. S2) respectively while that in the free receptor HL, they appear at a bit downfield position of 3.80 and 2.13 respectively (Fig. S3). The broad singlet at 13.56 ppm corresponding to –OH proton in the free ligand disappears in the complex suggesting the coordination of oxygen atom to the nickel center. The aromatic protons

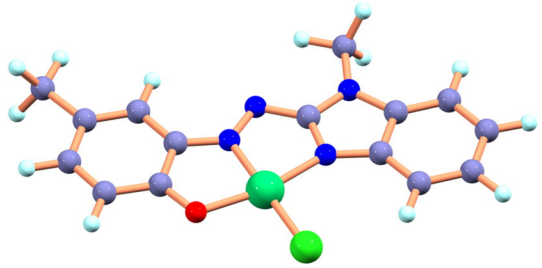

Fig. 6. Optimized structure of HL–Ni^{2+} complex by DFT/B3LYP method.

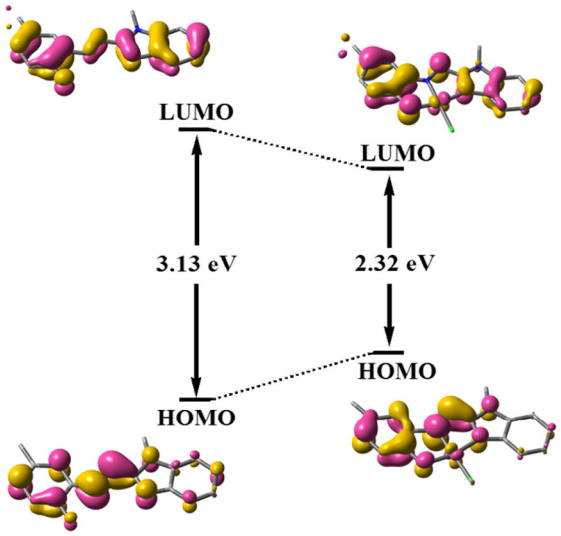

Fig. 7. Contour plots of HOMO, LUMO and HOMO–LUMO energy gap in HL and HL–Zn^{2+} complex.

in case of HL–Ni^{2+} complex, appear at a bit downfield region compared to that of the free receptor HL (Fig. S3).

3.3. Cation sensing studies of HL

3.3.1. UV–Vis study

The binding studies of receptor HL with different metal ions has been carried out in DMSO–HEPES buffer (1:1, v/v, pH 7.4) solution. Receptor HL (10 μM) shows an absorbance band at 403 nm. Addition of $NiCl_2$ (100 μM) solution causes decrease in intensity of the absorption band at 403 nm and a new absorption band appears at 600 nm with an isosbestic at around 500 nm (Fig. 1). This indicates the formation of a complex between the receptor HL and Ni^{2+}. Due to the complexation with Ni^{2+}, distinct color change occurs from orange yellow to blue (Fig. 2). Furthermore the sensing ability of HL with Ni^{2+} at different pH has also been studied. At lower pH, the receptor HL has no significant response to Ni^{2+} in absorption spectroscopy, may be due to protonation of the receptor HL. The absorbance at 600 nm is in maximum and almost constant in the pH range of 7.0 to 9.0, above pH 9.0, the absorbance is gradually decreased (Fig. 3). It indicates that the receptor may be suitable for biological applications at the physiological pH. UV–Vis spectrum of HL is also studied in the presence of other metals i.e. Ca^{2+}, Mg^{2+}, Mn^{2+}, Fe^{3+}, Al^{3+}, Cr^{3+}, Co^{2+}, Zn^{2+}, Cu^{2+}, Cd^{2+} and Hg^{2+} but no significant changes are observed in either of the cases (Fig. 4). Actually, the cavity of HL binds selectively with Ni^{2+} due to the proper size matching of the analyte with that of the binding site.

The selectivity of HL for Ni^{2+} is studied in the presence of other metal ions such as Ca^{2+}, Mg^{2+}, Mn^{2+}, Fe^{3+}, Al^{3+}, Cr^{3+}, Co^{2+}, Zn^{2+}, Cu^{2+}, Cd^{2+} and Hg^{2+}. The intensity of the absorption band at 600 nm due to formation of HL–Ni^{2+} complex is not at all disturbed due to the presence of other metal ions simultaneously in the solution (Fig. 5). Thus HL shows an excellent binding affinity for Ni^{2+} even in the presence of other metal ions and HL can detect Ni^{2+} very rapidly in other physiological samples where other metal ions like Ca^{2+}, Mg^{2+}, Mn^{2+}, Fe^{3+}, Al^{3+}, Cr^{3+}, Co^{2+}, Zn^{2+}, Cu^{2+}, Cd^{2+} and Hg^{2+} usually coexist with the analyte.

Job's plot reveals that the maximum absorption at 600 nm corresponds to mole fraction at 0.5 (Fig. S4), while intensity at 403 nm is minimized at mole fraction 0.5 (Fig. S5). Thus it clearly indicates that the complex formation between Ni^{2+} and HL has the stoichiometric ratio of 1:1. The mole ratio plot also reflects that the absorption intensity at 600 nm increases till the mole ratio of the analyte to the receptor HL reaches ~1.0, thus indicating 1:1 complex formation (Fig. S6).

From UV–Vis spectral change, limit of detection of the chemosensor for Ni^{2+}, is determined using the equation LOD = K × SD / S, where SD is the standard deviation of the blank solution and S in the slope of the calibration curve (Fig. S7). The limit of detection for Ni^{2+} is 0.14 μM from UV–Vis spectral titration. This result clearly demonstrates that the chemosensor is highly efficient in sensing Ni^{2+} even in very minute level. The association constant of Ni^{2+} for the receptor HL is found to be $2.074 \times 10^5\ M^{-1}$ (Fig. S8).

3.4. Electronic spectra and DFT calculation

To get detailed insight into the interaction of HL with Ni^{2+}, the DFT studies of the proposed square planar nickel complex has been carried out. In a square planar environment, three coordination sites are satisfied by the N, N, O donor of HL, and one site being occupied by a Cl^- (Fig. 6). The calculated N = N(azo) bond distance of the free receptor corresponding to 1.267 Å has been significantly enhanced to 1.298 Å in nickel complex, supporting coordination of azo-N to nickel center, while the C–O bond distance in HL decreased from 1.349 Å to 1.289 Å due to coordination. The proposed geometry is supported by mass spectral analysis of HL–Ni^{2+} complex and NMR studies.

The calculated energy and composition of selected molecular orbitals of Ni^{2+} complex are summarized in Table S1. Contour plots of selected molecular orbitals of HL–Ni^{2+} complex are given in Fig. S9. The HOMO–LUMO gap of HL is significantly decreased from 3.13 eV to 2.32 eV in Ni^{2+} complex and thus influenced the solution spectrum which is in good agreement with the red shift in solution spectra (Fig. 7).

The changes in electronic spectrum of HL upon complexation with Ni^{2+} have been interpreted by TDDFT calculations. In free receptor HL, the experimental bands at 403 nm and 282 nm correspond to HOMO → LUMO and HOMO-5 → LUMO + 1 transitions respectively (Table 1). In the complex, the low energy band has been observed at

Table 1
Vertical electronic transitions in HL calculated by TDDFT/B3LYP/CPCM method using DMSO as solvent.

$E_{excitation}$ (eV)	$\lambda_{excitation}$ (nm)	Osc. strength (f)	Key transitions	Character	$\lambda_{expt.}$ (nm)
2.7736	447.0	0.2528	(97%) HOMO → LUMO	$\pi \rightarrow \pi$	403
4.2158	294.1	0.1762	(69%) HOMO-5 → LUMO + 1	$\pi \rightarrow \pi^*$	282

Table 2
Vertical electronic transitions in HL–Ni^{2+} complex calculated by TDDFT/B3LYP/CPCM method using DMSO as solvent.

$E_{excitation}$ (eV)	$\lambda_{excitation}$ (nm)	Osc. strength (f)	Key transitions	Character	$\lambda_{expt.}$ (nm)
1.8642	665.1	0.0289	(83%) HOMO-4 → LUMO + 1	π(L) → dπ(Ni), LMCT	644
1.9860	624.3	0.1786	(79%) HOMO → LUMO	π(L) → π^*(L), ILCT	600
2.2737	545.3	0.0206	(69%) HOMO-5 → LUMO + 1	dπ(Ni) → dπ(Ni), d-d	562
3.0231	410.1	0.2022	(87%) HOMO-3 → LUMO	π(L) → π^*(L), ILCT	393

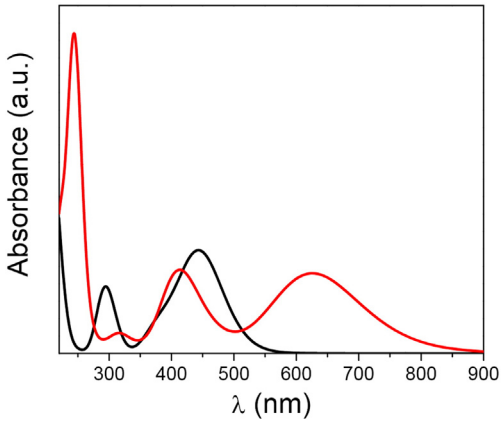

Fig. 8. Theoretical spectra of HL (—) and HL–Ni^{2+} complex (—) calculated by TDDFT/B3LYP/CPCM method using DMSO as solvent.

600 nm along with two shoulders at 644 nm and 562 nm. The intense band at 600 nm, corresponds to the calculated HOMO → LUMO transition at 624 nm with moderate oscillator strength, $f = 0.1786$, having ILCT character. The transitions at 644 nm (HOMO-4 → LUMO + 1) and 562 nm (HOMO-5 → LUMO + 1) correspond to the experimentally obtained weak transitions at 665 nm and 545 nm having LMCT and d-d character respectively. The band at 393 nm is well corroborated with the calculated transition at 410 nm having ILCT character for HOMO-3 → LUMO transition (Table 2). The changes in electronic spectra due to complex formation are also reflected in the theoretically calculated spectra of HL and HL–Ni^{2+} (Fig. 8).

4. Conclusion

The sensing ability of the receptor HL for Ni^{2+} has been extensively studied using UV–Vis spectroscopy. HL shows distinct color change from orange yellow to blue, visible under the naked eye, due to specific binding with nickel(II). Interference study also shows that HL is highly efficient in detecting Ni^{2+} over all other metal ions that commonly co-exist with Ni^{2+} in physiological and environmental samples. Thus HL provides a pathway for a very rapid, sensitive and selective detection of Ni^{2+}.

Acknowledgment

Financial supports received from the Department of Science and Technology, New Delhi, India (No. SB/EMEQ–242/2013) is gratefully acknowledged. D. Sarkar and A. K. Pramanik are thankful to CSIR, New Delhi, India for their fellowships.

Appendix A. Supplementary data

Supplementary data to this article can be found online at http://dx.doi.org/10.1016/j.saa.2015.08.052.

References

[1] M. Kumar, M. Bhalla, A. Dhir, J.N. Babu, Dalton Trans. 39 (2010) 10116–10121.
[2] E. Denkhaus, K. Salnikow, Crit. Rev. Oncol. Hematol. 42 (2002) 35–56.
[3] W. Lee, K.A. Davis, R.L. Rettmer, R.F. Labbe, Am. J. Clin. Nutr. 48 (1988) 286–290.
[4] X.Q. Liu, X. Zhou, X. Shu, J. Zhu, Macromolecules 42 (2009) 7634–7637.
[5] J.R. Sheng, F. Feng, Y. Qiang, F.G. Liang, L. Sen, F.H. Wei, Anal. Lett. 41 (2008) 2203–2213.
[6] H.X. Wang, D.L. Wang, Q. Wang, X.Y. Li, C.A. Schalley, Org. Biomol. Chem. 8 (2010) 1017–1026.
[7] L. Feng, Y. Zhang, L.Y. Wen, L. Chen, Z. Shen, Y.F. Guan, Analyst 136 (2011) 4197–4203.
[8] O. Haasw, M. Klarre, J.A.C. Broaekaert, K.K. Rothensee, Analyst 123 (1998) 1219–1222.
[9] C.E.C. Malgalhaes, F.J. Krug, A.H. Fostier, H.J. Berndt, Anal. Atom. Spectrom. 12 (1997) 1231–1234.
[10] D. Peralta-Domínguez, M. Rodríguez, G. Ramos-Ortíz, J. Luis Maldonadoa, M.A. Meneses-Navaa, O. Barbosa-Garcíaa, R. Santillan, N. Farfánc, Sensors Actuators B 207 (2015) 511–517.
[11] J. Jiang, C. Gou, J. Luo, C. Yi, X. Liu, Inorg. Chem. Commun. 15 (2012) 12–15.
[12] L. Wang, D. Ye, D. Cao, Spectrochim. Acta A 90 (2012) 40–44.
[13] S. Goswami, S. Chakraborty, S. Paul, S. Halder, A.C. Maity, Tetrahedron Lett. 54 (2013) 5075–5077.
[14] A. Khalafi-Nezhad, M.N. Soltani Rad, H. Mohabatkar, Z. Asrari, B. Hemmateenejad, Bioorg. Med. Chem. 13 (2005) 1931–1938.
[15] J. Mann, A. Baron, Y. Opoku-Boahen, E. Johansson, G. Parkinson, L.R. Kelland, S. Neidle, J. Med. Chem. 44 (2001) 138–144.
[16] J.L. Adams, J.C. Boehm, T.F. Gallagher, S. Kassis, E.F. Webb, R. Hall, M. Sorenson, R. Garigipati, D.E. Griswold, J.C. Lee, Bioorg. Med. Chem. Lett. 11 (2001) 2867–2870.
[17] R.K. Ujjinamatada, A. Baier, P. Borowski, R.S. Hosmane, Bioorg. Med. Chem. Lett. 17 (2007) 2285–2288.
[18] S.A.F. Rostom, H.M.A. Ashour, H.A.A.E. Razik, A.E.F.H.A.E. Fattah, N.N. El-Din, Bioorg. Med. Chem. 17 (2009) 2410–2422.
[19] F. Patzold, F. Zener, J.H. Heyer, H.J. Nichlas, Synth. Commun. 22 (1992) 281–288.
[20] J.J.V. Eynde, F. Delfosse, P. Lor, Y.V. Haverbeke, Tetrahedron 51 (1995) 5813–5818.
[21] K.J. Lee, K.D. Janda, Can. J. Chem. 79 (2001) 1556.
[22] H. Chikashita, S. Nishida, M. Miyazaki, Y. Morita, K. Itoh, Bull. Chem. Soc. Jpn. 60 (1987) 737–746.
[23] H. Goker, M. Alp, S. Yildiz, Molecules 10 (2005) 1377–1386.
[24] D. Sarkar, A.K. Pramanik, T.K. Mondal, Spectrochim. Acta A 115 (2013) 421–425.
[25] M.K. Paira, T.K. Mondal, D. Ojha, A.M.Z. Slawin, E.R.T. Tiekink, A. Samanta, C. Sinha, Inorg. Chim. Acta 370 (2011) 175–186.
[26] Gaussian 09, Revision D.01. M.J. Frisch, G.W. Trucks, H.B. Schlegel, G.E. Scuseria, M.A. Robb, J.R. Cheeseman, G. Scalmani, V. Barone, B. Mennucci, G.A. Petersson, H. Nakatsuji, M. Caricato, X. Li, H.P. Hratchian, A.F. Izmaylov, J. Bloino, G. Zheng, J.L. Sonnenberg, M. Hada, M. Ehara, K. Toyota, R. Fukuda, J. Hasegawa, M. Ishida, T. Nakajima, Y. Honda, O. Kitao, H. Nakai, T. Vreven, J.A. Montgomery Jr., J.E. Peralta, F. Ogliaro, M. Bearpark, J.J. Heyd, E. Brothers, K.N. Kudin, V.N. Staroverov, R. Kobayashi, J. Normand, K. Raghavachari, A. Rendell, J.C. Burant, S.S. Iyengar, J. Tomasi, M. Cossi, N. Rega, J.M. Millam, M. Klene, J.E. Knox, J.B. Cross, V. Bakken, C. Adamo, J. Jaramillo, R. Gomperts, R.E. Stratmann, O. Yazyev, A.J. Austin, R. Cammi, C. Pomelli, J.W. Ochterski, R.L. Martin, K. Morokuma, V.G. Zakrzewski, G.A. Voth, P. Salvador, J.J. Dannenberg, S. Dapprich, A.D. Daniels, Ö. Farkas, J.B. Foresman, J.V. Ortiz, J. Cioslowski, D.J. Fox, Gaussian, Inc., Wallingford CT, 2009.
[27] A.D. Becke, J. Chem. Phys. 98 (1993) 5648–5652.
[28] C. Lee, W. Yang, R.G. Parr, Phys. Rev. B 37 (1988) 785–789.
[29] T. Clark, J. Chandrasekhar, G.W. Spitznagel, P.V.R. Schleyer, J. Comput. Chem. 4 (1983) 294–301.
[30] P.J. Hay, W.R. Wadt, J. Chem. Phys. 82 (1985) 270–283.
[31] W.R. Wadt, P.J. Hay, J. Chem. Phys. 82 (1985) 284–298.
[32] P.J. Hay, W.R. Wadt, J. Chem. Phys. 82 (1985) 299–310.
[33] V. Barone, J. Chem. Phys. 120 (2004) 3059–3065.
[34] R. Bauernschmitt, R. Ahlrichs, Chem. Phys. Lett. 256 (1996) 454–464.
[35] R.E. Stratmann, G.E. Scuseria, M.J. Frisch, J. Chem. Phys. 109 (1998) 8218–8224.
[36] M.E. Casida, C. Jamorski, K.C. Casida, D.R. Salahub, J. Chem. Phys. 108 (1998) 4439–4449.
[37] V. Barone, M. Cossi, J. Phys. Chem. A 102 (1998) 1995–2001.
[38] M. Cossi, V. Barone, J. Chem. Phys. 115 (2001) 4708–4717.
[39] M. Cossi, N. Rega, G. Scalmani, V. Barone, J. Comput. Chem. 24 (2003) 669–681.